IEEE Access
Multidisciplinary | Rapid Review | Open Access Journal

Date of publication xxxx 00, 0000, date of current version xxxx 00, 0000.

Digital Object Identifier 10.1109/ACCESS.2017.Doi Number

A Novel Heap based Optimizer for Scheduling of Large-scale Combined Heat and Power Economic Dispatch

AHMED R. GINIDI[1], ABDALLAH M. ELSAYED[2], ABDULLAH M. SHAHEEN[1], EHAB E. ELATTAR[3] (SMIEEE), RAGAB A. EL-SEHIEMY[4] (SMIEEE)

[1] Electrical Engineering Department, Faculty of Engineering, Suez University, Suez 43533, Egypt
[2] Electrical Engineering Department, Faculty of Engineering, Damietta University, Damietta 34517, Egypt
[3] Electrical Engineering Department, College of Engineering, Taif University, Taif 21944, Saudi Arabia
[4] Electrical Engineering Department, Faculty of Engineering, Kafrelsheikh University, Kafrelsheikh 33516, Egypt

Corresponding author: Ragab A. El-Sehiemy (e-mail: elsehiemy@eng.kfs.edu.eg)

This work was supported by Taif University Researchers Supporting Project number (TURSP-2020/86), Taif University, Taif, Saudi Arabia.

ABSTRACT Cogeneration systems economic dispatch (CSED) provides an optimal scheduling of heat /power generating units. The CSED aims to minimize the whole fuel cost (WFC) of the cogeneration units taking into consideration their technical and operational limits. Then, the current paper examines the first implementation of dominant bio-inspired metaheuristic called heap-based optimization algorithm (HBOA). The HBOA is powered by an adaptive penalty functions for getting the optimal operating points. The HBOA is inspired from the organization hierarchy, where the mechanism consists of the interaction among the subordinates and their immediate boss, the interaction among the colleagues, and the employee's self-contribution. Based on the infeasible solutions' remoteness from the nearest feasible point, HBOA penalizes them with various degrees. Four case studies of the CSED are implemented and analyzed, which comprise of 4, 24, 84 and 96 generating units. The HBOA is proposed to solve CSED problem with consideration of transmission losses and the valve point impacts. An investigation with the recent optimization algorithms, which are supply demand optimization (SDO), jellyfish search optimization algorithm (JFSOA), and marine predators' optimization algorithm (MPOA), the improved MPOA (IMPOA) and manta ray foraging (MRF), is developed and elaborated. From the obtained results, it is clearly observed that the optimal solutions gained, in terms of WFC, reveal the feasibility, capability, and efficiency of HBOA compared with other optimizers especially for large-scale systems. case

INDEX TERMS Cogeneration systems economic dispatch, fuel cost minimization, heap based optimization algorithm, distribution reconfiguration, valve point impacts, transmission losses.

Nomenclature:

a_i, b_i, & c_i	The i^{th} power plant cost coefficients
a_j; b_j, & c_j	The j^{th} heat plant cost coefficients
a_k, b_k, c_k, d_k, e_k & f_k	The k^{th} unit cost coefficients
C	Total production costs
$C_i(P_i^p)$	Fuel cost of power unit i
$C_j(H_j^h)$	Fuel cost of j^{th} heat plant
$C_k(P_k^c, H_k^c)$	Operational cost of k^{th} cogeneration unit
H_d	Heat demand in the system
N_p , N_h and N_c	Number of power-only plants, heat-only plants and cogeneration units
P	Output of power generation units
P_d	Electric power demand
P_{Loss}	Transmission losses
λ_i & ρ_i	Valve-point cost coefficients
H	Output of heat generation units

This article has been accepted for publication in a future issue of this journal, but has not been fully edited. Content may change prior to final publication. Citation information: DOI 10.1109/ACCESS.2021.3087449, IEEE Access

I. INTRODUCTION

A. MOTIVATION AND INCITEMENT

Conversion from fossil fuels to electricity in the conventional units are the main cause for low energy efficiency of these units that leads to significant wasted energy amount. However, cogeneration systems economic dispatch (CSED) can save up to 40% of the generation costs, and achieve 90% energy efficiency [1]. Additional advantage of cogeneration units for the environment is the associated decrease in contaminating gas emissions, which is generally assessed by 13–18% [1]. The importance of CSED is evident in achieving the minimum operating costs of cogeneration units with optimum scheduling of heat and power units as well with keeping of operational constraints, which are heat and power balance constraint, valve-point effect, and generation capacity limits which take into consideration combined heat and power (CHP) units' non-convex feasible operating areas. With the growing size, CSED has become a distinctive non-convex, non-linear, and large-scale global optimization issue in the viewpoint of theories and engineering applications [1].

B. LITERATURE REVIEW

A plethora of conventional and mathematical approaches have been developed to solve CSED optimization problem such as sequential quadratic programming (SQP) [2], lagrangian relaxation (LR) [3], benders decomposition (BD) [4] and LR with surrogate subgradient (LRSS) multiplier updates [5]. These optimization techniques may converge to a local optimum, which is highly dependent on the initial starting points. Furthermore, the inclusion of more non-convexity, non-linear, and non-smooth cost functions increases the complexity of many of them [3], [6].

Nowadays, various efficient heuristic and meta-heuristic optimization algorithms have been developed to the CSED problem for their capability of dealing with such complex problem. The researchers have employed many optimization algorithms for achieving the best possible scheduling of heat and electricity producing units with least cost such as whale optimization algorithm (WOA) [7], harmony search (HS) [8], differential evolution (DE) algorithm [9], quantum optimization (QO) [10], and particle swarm optimization (PSO) [11]. A hybrid PSO and weighted vertices based (WVO), has been applied in [12] to obtain the optimal solution of CSED problem. In [13], particle swarm optimization with time-varying acceleration coefficients (TVAC-PSO) has been employed with adding a sinusoidal term to the polynomial cost function to represent the effect of the valve point. The objective function of pollutant gas emissions was combined with the operational cost to generate a multi-objective CSED issue to be addressed in [14]. In [15], PSO was used to simulate the functioning of a coal-fired CSED that was coupled to heat and power generating units. In [16], the security of the electricity network was examined in a multi-objective formulation used for CSED management, which takes into account the cost of pollutant emissions. The CSED problem while retaining the dependability of micro-grids and operational restrictions was provided in [17].

Moreover, multi-player harmony search (MPHS) [18], oppositional teaching learning-based optimizer (OTLBO) [19], line-up competition optimizer [20], non-dominated sorting genetic algorithm (NSGA) [21], bee colony optimization (BCO) [22], salp swarm algorithm (SSA) [23], multi-verse optimizer (MVO) [24], equilibrium optimizer (EO) [25], and stochastic fractal search algorithm [26], [27]. have been presented to solve this problem with lesser computational effort.

In [28], a cuckoo search optimization, with emerged sorting process in a descending order based on the fitness value and new operator to update the individuals, has been applied for the CSED problems. In [29], an improved genetic algorithm with two types of crossover operators for the CSED issue. As well, hybrid non-dominated sorting genetic algorithm with multi-objective PSO [30], multi-verse optimization (MVO) [24], and an enhanced shuffle frog leaping optimizer [31] have been efficiently applied for the same purpose but their validations were restricted to just small-scale applications of 5-units and 7-units systems. In [32], a novel Kho-Kho Optimization (KKO) for tackling the CSED challenge was described, although it requires a feasibility assessment because several obtained operational points did not meet their given limitations. Squirrel search algorithm (SSA) has been employed for solving complicated multi-region combined heat and power economic dispatch problem with consideration of thermal generators and solar and wind power uncertainty [33].

Efforts have not ceased to get new reliable and effective techniques and develop the existing techniques for optimal solution of such complex problems [34]. One of these new effective optimization techniques is the heap-based optimization algorithm (HBOA). HBOA is inspired from the organization hierarchy. This can be seen when a team working for achieving their goal arrange themselves in a hierarchy which is named corporate rank hierarchy (CRH) to organize the search agents based on their fitness in a hierarchy using the heap data structure.

C. CONTRIBUTION AND PAPER ORGANIZATION

The paper presents a solution to the combined heat and power economic dispatch problem using a heap-based optimizer. The objective is to find the optimal schedule of generating units such that heat and power, both demands are met from cogeneration units, in an optimal manner. In this paper, HBOA is developed to solve the CSED issue while considering the valve point effects and other practical restrictions. This paper contributions are reviewed as:

- HBOA is designed with an adapted penalty formulas to find an optimal feasible operating coordinate for the

This article has been accepted for publication in a future issue of this journal, but has not been fully edited. Content may change prior to final publication. Citation information: DOI 10.1109/ACCESS.2021.3087449, IEEE Access

CSED complex problem. Based on the distance between the infeasible option and the next feasible option, HBOA penalizes them with various degrees, which give it the opportunity to easily reach optimal solutions even in complex problems.

- The CSED model is inspected considering valve point impacts and transmission losses.
- HBOA is effectively employed with high superiority to previous techniques on small-scale systems such as the 4-units, and 24-unit systems with technical and operational constraints fulfillment.
- HBOA feasibility, scalability and validity are verified and assessed for large-scale systems such as the 84-unit and 96-unit systems.
- For all systems and studied cases, HBOA improves the solution quality and capability of finding feasible optimal operating points of all units (heat only units, power only units and cogeneration units).

The remaining of the paper is organized as follows: The CSED problem is illustrated in Section II. Additionally, in Section III, HBOA is described for obtaining the optimal CSED solution. In Section IV, the simulation results and discussion are introduced. Finally, Section V concludes this work.

II. PROBLEM FORMULATION

The main objective of the CSED problem aims to minimize the whole fuel costs (WFC) supplying the cogeneration, heat only and power only units that satisfy the power and heat demands. This can be represented as follows [1]:

$$\text{Min}\sum_{i=1}^{N_p} C_i P_i^p + \sum_{j=1}^{N_h} C_j H_j^h + \sum_{k=1}^{N_C} C_k (P_k^C, H_K^C) \quad (\$/\text{h}) \tag{1}$$

The terms of generation costs given in Eq. (1) can be written as follows [7]:

$$C_i(P_i^p) = a_i (P_i^p)^2 + b_i P_i^p + c_i + \left|\lambda_i \sin(\rho_i (P_i^{p_{\min}} - P_i^p))\right| \quad (\$/\text{h}) \tag{2}$$

$$C_j(H_j^h) = a_j (H_j^h)^2 + b_j P_j^p + c_j \quad (\$/\text{h}) \tag{3}$$

$$C_k(P_k^c, H_k^c) = a_k (P_k^c)^2 + b_k P_k^p + c_k + d_k (H_k^c)^2 + e_k H_k^c + f_k H_k^c P_k^c \quad (\$/\text{h}) \tag{4}$$

The cost function of power-only plant is described in Eq. (2) which comprises a quadratic and sinusoidal terms, where the sinusoidal term manifests the valve-point impacts. The valve point impacts make the CSED as non-differentiable and non-convex problem. The cost of heat only is represented in Eq. (3). Additionally, for Eq. (4) represents the cogeneration units cost function, where the H^c and P^c are the heat output and power output, respectively.

The CSED problem could be optimized with subject to the following constraints for feasible solutions:

$$\sum_{i=1}^{N_p} P_i^p + \sum_{j=1}^{N_c} P_j^c = P_d \tag{5}$$

$$\sum_{j=1}^{N_c} H_j^c + \sum_{k=1}^{N_h} H_k^h = H_d, \tag{6}$$

$$P_i^{p_{\min}} \le P_i^p \le P_i^{p_{\max}} \quad i = 1,\ldots,N_p, \tag{7}$$

$$H_j^{h_{\min}} \le H_j^h \le H_j^{h_{\max}} \quad j = 1,\ldots,N_h, \tag{8}$$

$$P_k^{c_{\min}}(H_k^c) \le P_k^c \le P_k^{c_{\max}}(H_k^c) \quad k = 1,\ldots,N_c, \tag{9}$$

$$H_k^{c_{\min}}(P_k^c) \le H_k^c \le H_k^{c_{\max}}(P_k^c) \quad k = 1,\ldots,N_c, \tag{10}$$

Equation (5) illustrates the balance of power generation and demand. Equation (6) manifests the heat generation and demand balance. Moreover, power-only plants capacity limits are demonstrated in Eq. (7), whereas Eq. (8) shows the heat-only units generation limits. Additionally, the cogeneration units' capacity limits are described in Eqs. (9) and (10).

The transmission losses are added to the power balance constraint, which introduces extra non-linearities into the model. It can be evaluated as signified in Eq. (11) [35]. Therefore, the equality balance constraint of Eq. (5) could be changed as characterized in Eq. (12).

$$P_{Loss} = \sum_{i=1}^{N_p}\sum_{m=1}^{N_p} B_{im} P_i^p P_m^p + \sum_{i=1}^{N_p}\sum_{j=1}^{N_c} B_{ij} P_i^p P_j^c + \sum_{j=1}^{N_c}\sum_{n=1}^{N_c} B_{in} P_j^c P_n^c \tag{11}$$

$$\sum_{i=1}^{N_p} P_i^p + \sum_{j=1}^{N_c} P_j^c = P_d + P_{Loss} \tag{12}$$

III. HEAP BASED OPTIMIZATION ALGORITHM FOR CSED problem

The heap-based algorithm is inspired from organizations hierarchy. This can be seen when a team working arrange themselves in a hierarchy for achieving their goal, which is named corporate rank hierarchy (CRH). In this regard, the concept of CRH is to organize the search agents based on their fitness in a hierarchy using the heap data structure to map this concept. Three elements are the main pillars of HBOA. The first element is the collaboration among the assistants and their immediate boss. While the second element is the interaction among the colleagues. The third element is the self-contribution of the employees. Four steps are developed for mapping the heap concept as follows:

A. MODELING THE CORPORATE RANK HIERARCHY

The CRH model is developed with the heap data structure which is similar to tree-shaped data structure. Therefore, the full CRH manifests the population while the search agent represents a heap node. The search agent's fitness is the master of the heap node, and the population index of the search agent is the value of the heap node.

This article has been accepted for publication in a future issue of this journal, but has not been fully edited. Content may change prior to final publication. Citation information: DOI 10.1109/ACCESS.2021.3087449, IEEE Access

B. FIRST PILLAR: MODELING OF THE INTERACTION WITH IMMEDIATE BOSS

In the centralized organizational structure, the policies and rules are set from the upper levels, whereas subordinates must execute the instruction from their direct supervisors. It can be described through updating the agent position of each search using the following equation:

$$x_i^k(t+1) = B^k + \gamma(2r-1)\left|B^k - x_i^k(t)\right| \tag{13}$$

where; t indicates the current iteration, k signifies the k^{th} vector component of, and $|\ |$ refers to the absolute value. The term $(2r-1)$ represents the k^{th} component of vector $\vec{\lambda}$, which is produced randomly as illustrated in Eq. (14):

$$\lambda^k = 2r-1 \tag{14}$$

where; r exemplifies a random number from the range [0,1] which is generated according to uniform distribution. However, γ is calculated according to Eq. (15).

$$\gamma = \left| 2 - \frac{(t \bmod \frac{T}{C})}{\frac{T}{4C}} \right| \tag{15}$$

where; T exemplifies the total iterations' number, and C is a user-defined parameter which controls the variation in the values of $\gamma(2r-1)$. However, the parameter C will complete in T iterations and can be represented as follows:

$$C = \lfloor T/25 \rfloor \tag{16}$$

C. THE SECOND PILLAR: MATHEMATICAL MODELING OF THE INTERACTION BETWEEN COLLEAGUES

The colleagues with the same level are considered as the nodes and each agent $\vec{x_i}$ updates its position with respect to its randomly designated colleague $\vec{S_r}$:

$$x_i^k(t+1) = \begin{cases} S_r^k + \gamma\lambda^k\left|S_r^k - x_i^k(t)\right|, & f(\vec{S_r}) < f(\vec{x_i}(t)) \\ x_i^k + \gamma\lambda^k\left|S_r^k - x_i^k(t)\right|, & f(\vec{S_r}) \geq f(\vec{x_i}(t)) \end{cases} \tag{17}$$

where; f describes the fitness of the search agent.

D. THE THIRD PILLAR: MODELING OF THE SELF-CONTRIBUTION OF AN EMPLOYEE

The self-contribution of an employee is mapped in this phase as manifested in the following equation:

$$x_i^k(t+1) = x_i^k(t) \tag{18}$$

E. MERGING THE THREE PILLARS

This subsection shows the merging procedure of the position updating equations into one equation. The probabilities of selection use a roulette wheel to balance both exploration and exploitation through splitting the proportions into p_1; p_2, and p_3. The selection of the proportion p_1 enables a search agent to update its position using Eq. (18), where the bound of p_1 can be calculated as follows:

$$p_1 = 1 - \frac{t}{T} \tag{19}$$

The selection of the proportion p_2 enables a search agent to update its position using Eq. (13), where the bound of p_2 can be calculated as follows:

$$p_2 = p_1 + \frac{1-p_1}{2} \tag{20}$$

The selection of the proportion p_3 enables a search agent to update its position using Eq. (17), where the bound of p_3 can be calculated as follows:

$$p_3 = p_2 + \frac{1-p_1}{2} = 1 \tag{21}$$

Consequently, Eq. (22) presents a general position updating mechanism of HBOA as follows:

$$x_i^k(t+1) = \begin{cases} x_i^k(t), & p \leq p_1 \\ B^k + \gamma\lambda^k\left|B^k - x_i^k(t)\right|, & p_1 < p < p_2 \\ S_r^k + \gamma\lambda^k\left|S_r^k - x_i^k(t)\right|, & p_2 < p \leq p_3 \text{ and } f(\vec{S_r}) < f(\vec{x_i}(t)) \\ x_r^k + \gamma\lambda^k\left|S_r^k - x_i^k(t)\right|, & p_2 < p \leq p_3 \text{ and } f(\vec{S_r}) \geq f(\vec{x_i}(t)) \end{cases} \tag{22}$$

where p represents a produced randomly number [0,1].

To handle the CSED problem, the HBOA is illustrated in Fig. 1. For mutual-dependent cogeneration units, the second form is shown in Fig. 2. Depending upon on penalty component inside the fitness under consideration, they are dealt utilizing quadratic penalized terms. As a result, the whole objective to be minimized (F) is formally defined as shown in (23):

$$\mathrm{F} = \mathrm{TF}C + \psi_{\mathrm{v}} \sum_{k=1}^{N_C} BI \,.\, \{P_k^C(H_k^C) - P_k^{CLimit}(H_k^C)\} \tag{23}$$

where; the term $(P_k^{CLimit}(H_k^c))$ reflects the power limit to the set heating output for the cogeneration (k). Moreover, the symbol (BI) manifests a binary coefficient which equals 1 for violation state and zero else, whilst ψ_{v} shows a penalized factor related to the cogeneration operating point violation ($\psi_{\mathrm{v}} = 50000$).

This article has been accepted for publication in a future issue of this journal, but has not been fully edited. Content may change prior to final publication. Citation information: DOI 10.1109/ACCESS.2021.3087449, IEEE Access

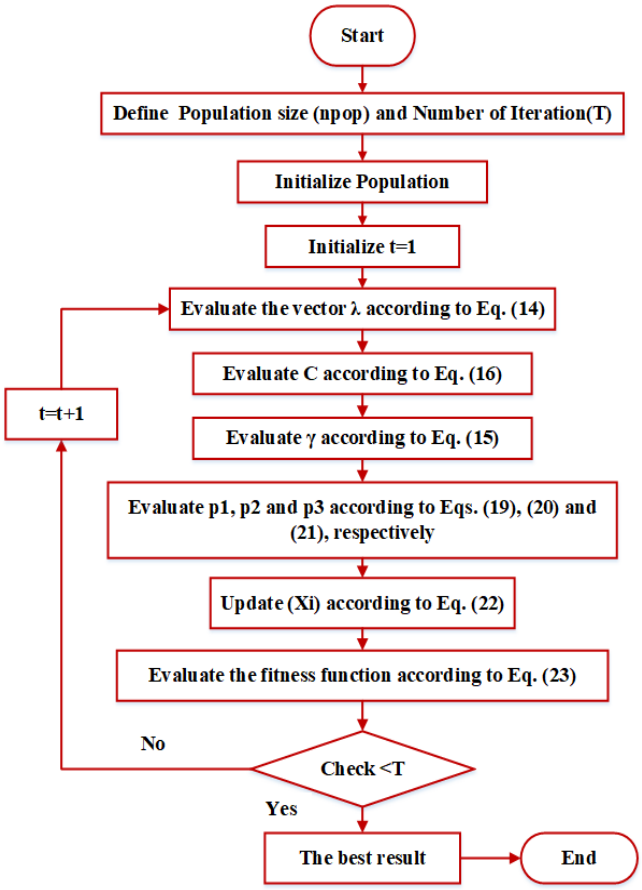

FIGURE 1. **Flowchart of the developed HBOA.**

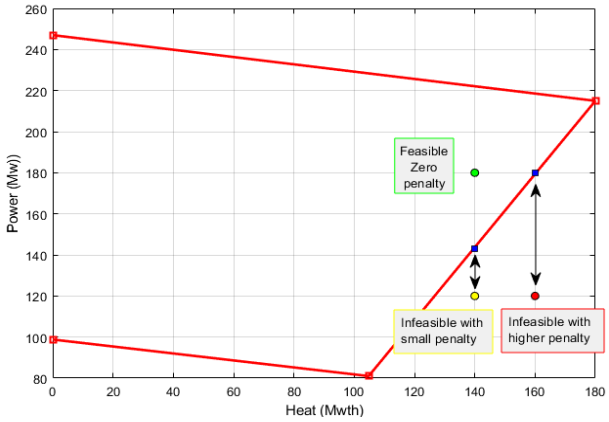

FIGURE 2. **Dependency between power and heat for cogeneration unit.**

It is illustrated according to Eq. (23) and Fig. 2, the value of the penalized component increases as the infeasible points are moved away from the next regarding borders. As a result, the HBOA provides a greater capacity for searching for viable sites. Furthermore, a stopping criterion is implemented in which the optimum result is acquired when a specified number of iterations is attained. Based on the infeasible solutions' distance from the next border, HBOA penalizes them with various degrees.

IV. SIMULATION RESULTS

In this section, the HBOA is applied on four test systems, which are 4-units, 24-unit, 84-unit and 96-unit test systems. The number of iterations (T) and individuals (n_{pop}) are 300 and 50, respectively, for the 4-units' systems while they are 3000 and 100, respectively, for the 24-unit, 84-unit and 96-unit systems.

A. THE 4-UNIT TEST SYSTEM

It involves single conventional power-only unit, two cogeneration units and one heat-only unit. The system demands of power and heat are 200 MW and 115 MWth, respectively [36]. The proposed HBOA optimizer is implemented and tested for optimal solution of CSED optimization problem and compared with other efficient mathematical approaches such as LR [3], SQP [2], LRSS [5] and BD [4] as depicted in Table 1. Additionally, recent techniques such as manta ray foraging (MRF) [37], jellyfish search optimization algorithm (JFSOA) [34], and supply demand optimization (SDO) are applied for fair comparison. As shown, from the obtained results, the effectiveness and robustness of the employed HBOA optimizer are demonstrated with a minimum WFC of 9257.0694 $. Ultimately, from the economic perspective, the yearly savings with the application of the proposed HBOA as compared with the WFC obtained by other conventional methods, LR [3], SQP [2], LRSS [5] and BD [4], is about 268.056 $/year. The convergence characteristics, shown in Fig. 3, clearly shows that HBOA is capable to find feasible operating points of all units and to improve the solution quality with respect to the recent techniques such as MRF[37], SDO and JFSOA.

B. SIMULATION RESULTS OF THE 24-UNIT TEST SYSTEM

The load and heat demand of this test system are respectively 2350 MW and 1250 MWth. Additionally, it includes 5 heat units, 13 thermal units, and 6 CHP units as obtained from [38]. The proposed HBOA is implemented and applied on this test system as tabulated in Table 2. By simulating the results, it can be observed that the HBOA gives optimal solution with WFC of 57994.51 $. Other reported techniques such as grey wolf optimization (GWO) [38], teaching learning-based optimization (TLBO) [19], oppositional TLBO (OTLBO) [19], group search optimization (GSO) [39], improved version of GSO (IGSO) [39], TVAC-PSO [13] and CPSO [13] are also applied, which give WFC of 57846.84 $, 58006.999 $, 57856.2676 $, 58225.745 $, 58049.01 $, 58122.746 $ and 59736.2635 $, respectively. Also, recent techniques MRF, SDO and JFSOA are applied on this test system which give WFC of 58173.93 $, 58208.0267 $ and 58739.5241 $, respectively. It is observed from the reported WFC (WFC^R) given in this table that the WFC obtained from GWO, TLBO and OTLBO overwhelmed the proposed HBOA for achieving minimum costs. However, by verifying the operating points of these methods, great violation of the operating point of CHP unit-6 is detected as shown in Figs.

This article has been accepted for publication in a future issue of this journal, but has not been fully edited. Content may change prior to final publication. Citation information: DOI 10.1109/ACCESS.2021.3087449, IEEE Access

4, 5 and 6 for GWO, TLBO and OTLBO techniques, respectively. As shown in these figures the operating point of CHP unit-6 is (31.47 MW and 18.39 MWth), (31.46 MW and 18.38 MWth), and (31.98 MW and 18.22 MWth) for GWO, TLBO and OTLBO, respectively. In addition, it is observed that small deviation between calculated WFC (WFC^C) and the reported value. Accordingly, the comparison of the proposed method with the GWO, TLBO and OTLBO techniques, in this case, is not fair comparison. While, in comparison with other techniques given in Table 2, the proposed method is considered the best.

Fig. 7 shows the convergence rates of the proposed technique and other recent optimization techniques. It is clear from this figure that HBOA is capable to find feasible operating points of all units and to improve the solution quality and finally reach the least WFC of 287933.8131$. In addition, achieving all constraints with 100% accuracy.

C. SIMULATION RESULTS OF 84-UNIT TEST SYSTEM

The load and heat demand of this the 84-unit system are 12700 MW and 5000 MWth, respectively. Additionally, it includes 20 heat units, 40 thermal units, and 24 CHP units as obtained from [7]. Table 3 gives the optimal unit scheduling using the proposed techniques as well as other relevant techniques. By simulating the result, it is observed that the obtained optimal solution achieved by HBOA is lower than the reported techniques which are WOA [7] and MPHS [18] as well as the recent techniques applied in this article which are MPOA, IMPOA, MRF, SDO and JFSOA.

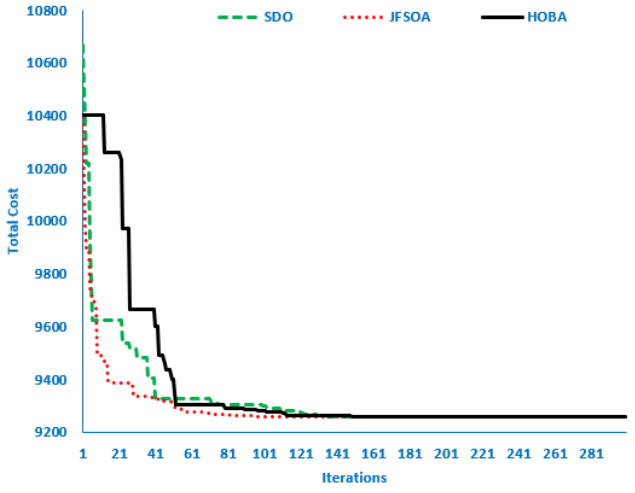

FIGURE 3. Convergence rates of HBOA versus other recent techniques for the CSED of 4-units system.

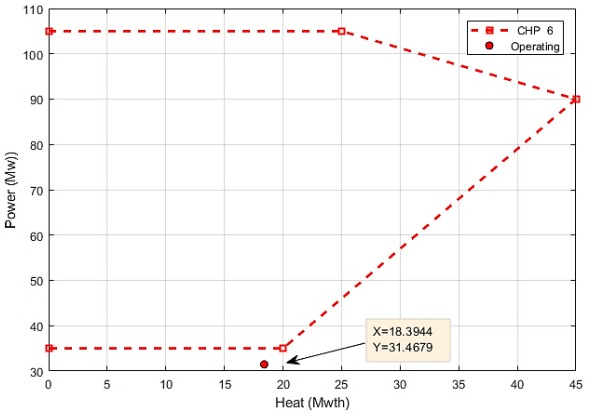

FIGURE 4. GWO based operating point of CHP unit-6 of the 24-unit test system [38].

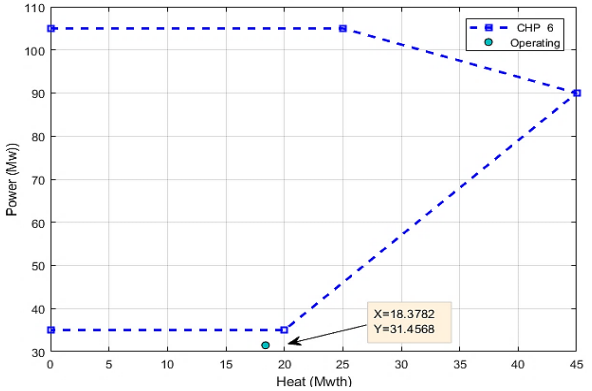

FIGURE 5. TLBO based operating point of CHP unit-6 of the 24-unit test system [19].

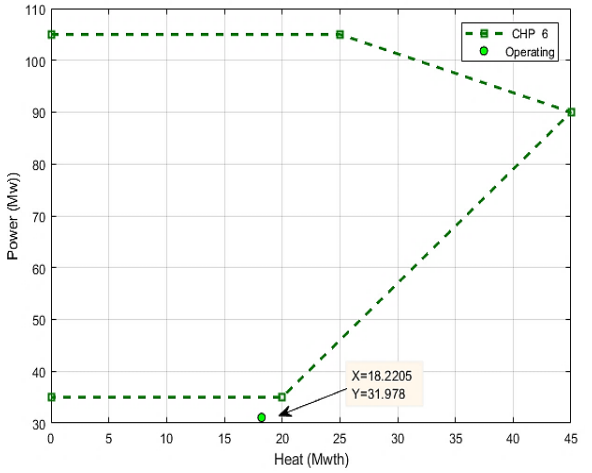

FIGURE 6. OTLBO-based operating point of CHP unit-6 of the 24-unit test system [19].

TABLE 1. Optimal schedluing of CSED problem for the 4-units system using HBOA and other techniques.

Unit	LR [3]	SQP [2]	BD [4]	LRSS [5]	MRF	JFSOA	SDO	HBOA
Pg1 (MW)	0	0	0	0	0	0	0	0
Pg2 (MW)	160	160	160	160	160	160	160	160
Hg2 (MWth)	40	40	40	40	40	40	40	40
Pg3 (MW)	40	40	40	40	39.9991	39.9991	39.9991	39.9991
Hg3 (MWth)	75	75	75	75	75.0009	75.0009	75.0009	75.0009
Hg4 (MWth)	0	0	0	0	0	0.0000	0.0000	0.0000
WFC ($)	**9257.1**	**9257.1**	**9257.1**	**9257.1**	**9257.0694**	**9257.0694**	**9257.0698**	**9257.0694**

This article has been accepted for publication in a future issue of this journal, but has not been fully edited. Content may change prior to final publication. Citation information: DOI 10.1109/ACCESS.2021.3087449, IEEE Access

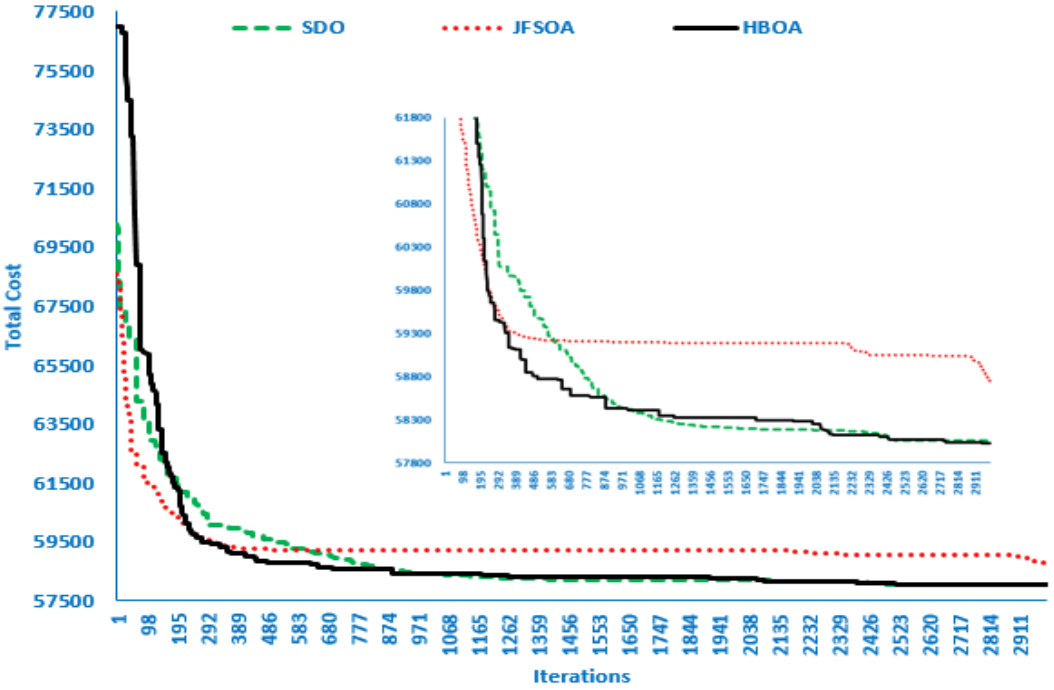

FIGURE 7. Convergence characteristics of HBOA versus other recent optimizaion techniques for the CSED problem of the 24-unit system.

TABLE 2. Optimal solution of CSED problem of the 24-unit system using HBOA and other techniques.

Unit	GWO[38]	TLBO [19]	OTLBO [19]	GSO [39]	IGSO [39]	TVAC-PSO [13]	CPSO [13]	MRF	JFSOA	SDO	HBOA
Pg1 (MW)	538.844	628.324	538.5656	627.7455	628.152	538.5587	680	538.5601	538.0895	449.2756	538.55874
Pg2 (MW)	299.3423	227.3588	299.2123	76.2285	299.4778	224.4608	0	149.1049	224.8625	149.6789	300.2175
Pg3 (MW)	299.3423	225.9347	299.122	299.5794	154.5535	224.4608	0	224.2988	301.8762	202.5620	301.08255
Pg4 (MW)	109.9653	110.3721	109.992	159.4386	60.846	109.8666	180	109.8616	158.7306	109.8603	159.77792
Pg5 (MW)	109.9653	110.2461	109.9545	61.2378	103.8538	109.8666	180	159.4583	110.5483	109.9316	63.217359
Pg6 (MW)	109.9653	160.1761	110.4042	60	110.0552	109.8666	180	109.8041	112.2867	159.7364	60.688902
Pg7 (MW)	109.9653	108.3552	109.8045	157.1503	159.0773	109.8666	180	109.8188	107.4217	160.0083	160.20652
Pg8 (MW)	109.9653	110.5379	109.6862	107.2654	109.8258	109.8666	180	159.5256	109.6984	159.7429	111.5383
Pg9 (MW)	109.9653	110.5672	109.8992	110.1816	159.992	109.8666	180	109.7499	109.9874	109.8345	161.25395
Pg10 (MW)	77.6223	75.7562	77.3992	113.9894	41.103	77.521	50.4304	76.9438	77.0731	77.3900	40
Pg11 (MW)	77.6223	41.8698	77.8364	79.7755	77.7055	77.521	50.5304	75.4655	41.9398	77.4070	40.000265
Pg12 (MW)	55	92.4789	55.2225	91.1668	94.9768	120	55	92.196	58.4508	92.3672	55.657936
Pg13 (MW)	55	57.514	55.0861	115.6511	55.7143	120	55	91.88	91.8472	92.3952	55.284532
Pg14 (MW)	83.465	82.5628	81.7524	84.3133	83.9536	88.3514	117.4854	85.705	81.9727	115.8210	87.944171
Pg15 (MW)	40	41.4891	41.7615	40	40	40.5611	45.9281	50.039	42.2700	40.9645	41.266255
Pg16 (MW)	82.7732	84.771	82.273	81.1796	85.7133	88.3514	117.4854	100.9829	83.4650	114.8737	84.034893
Pg17 (MW)	40	40.5874	40.5599	40	40	40.5611	45.9281	40.4323	41.8894	69.3012	43.143673
Pg18 (MW)	10	10.001	10.0002	10	10	10.0245	10.0013	10.0284	12.2384	10.1338	11.082469
Pg19 (MW)	31.4568	31.0978	31.4679	35.097	35	40.4288	42.1109	56.1452	45.3522	48.7160	35.044029
Hg14 (MWth)	106.0991	105.6717	105.2219	106.6588	106.4569	108.9256	125.2754	107.4333	104.5803	124.2764	108.69733
Hg15 (MWth)	75	76.2843	76.5205	74.998	74.998	75.4844	80.1174	83.6669	76.6280	75.7112	76.092716
Hg16 (MWth)	105.789	106.9125	105.5142	104.9002	107.4073	108.9256	125.2754	116.0123	104.7995	123.8075	106.47627
Hg17 (MWth)	75	75.5061	75.4833	74.998	74.998	75.484	80.1174	75.3723	75.5878	100.2936	77.714606
Hg18 (MWth)	40	39.9986	39.9999	40	40	40.0104	40.0005	40.0026	40.9191	40.0036	40.464341
Hg19 (MWth)	18.3782	18.2205	18.3944	19.7385	20	22.4676	23.2322	29.6101	24.5560	26.2104	20.020468
Hg20 (MWth)	469.7337	468.2278	468.9043	469.3368	466.2575	458.702	415.9515	437.9153	463.4714	399.9754	460.53781
Hg21 (MWth)	60	59.9867	59.9994	60	60	60	60	59.994	59.9228	59.9258	60
Hg22 (MWth)	60	59.9814	59.9999	60	60	60	60	59.9953	59.9511	59.9020	60
Hg23 (MWth)	120	119.6074	119.9854	119.6511	120	120	120	119.9982	119.6168	119.9138	119.99644
Hg24 (MWth)	120	119.603	119.9768	119.7176	119.8823	120	120	119.9996	119.9674	119.9803	120
Sum(Pg)	2350.26	2350	2350	2350	2350	2350.0002	2349.9	2350	2350.0000	2350.0000	2350.00
Sum(Hg)	1250	1250	1250	1250	1250	1250	1250	1250	1250.0000	1250.0000	1250.00
WFC^R	57846.84	58006.999	57856.2676	58225.745	58049.01	58122.746	59736.2635	58173.93	58208.0267	58739.5241	57994.51
WFC^C	57851.76*	58007*	57856.26*	58225.74	58048.56	58122.7494	59733.8271	58173.93	58208.0267	58739.5241	57994.51
Deviation	4.92	0.0008	0.0076	0.005	0.45	0.0034	2.4364	-	-	-	-

The superscript "R" refers to reported value and the superscript "C" refers to calculated value

This article has been accepted for publication in a future issue of this journal, but has not been fully edited. Content may change prior to final publication. Citation information: DOI 10.1109/ACCESS.2021.3087449, IEEE Access

In addition to that, an assessment of the operating points introduced in Table 3, it is found that the results reported by WOA [7] and MPHS [18] include a great violation on the operating point of many units. It is clearly observed from this assessment that the operating points of CHP units 42, 44, 45, 50-53 and 58-63, which obtained by WOA [7], are outside their acceptable limits. Fig 8 shows sample of violated operating points of CHP units 58-60. Also, the operating points provided by MPHS [18] for CHP units 43-45, 47, 50-52, 53, 55 and 59-62 are outside their acceptable limits. Fig. 9 provides sample of violated operating points of CHP units 58-60. The convergence characteristics shown in Fig. 10 manifest the superiority, stability and efficiency of the HBOA in finding feasible operating points of all the units and to improve the solution quality in this large system with all constraints achievement.

TABLE 3. Optimal scheduling results of CSED problem of 84-unit system using HBOA and other techniques.

Unit	WOA [7]	MPHS [18]	MPOA	IMPOA	MRF	JFSOA	SDO	HBOA
Pg1 (MW)	110.8794	113.9557	111.4996	111.8429	110.8514	111.1626385	113.5593533	113.9999976
Pg2 (MW)	112.2931	113.2521	113.9898	113.4366	112.3562	112.5520392	109.0508668	113.115563
Pg3 (MW)	98.1159	98.8762	106.8479	97.7637	100.7567	107.7765112	100.2258404	103.8372469
Pg4 (MW)	129.8682	179.7497	180.728	182.4321	140.3075	179.7375644	162.4975687	184.8069538
Pg5 (MW)	88.6586	95.803	96.9592	93.9162	91.0444	87.78776144	91.53858887	89.50520793
Pg6 (MW)	139.9998	140	106.125	139.9973	139.9861	139.9948775	106.3733811	106.6482728
Pg7 (MW)	196.1145	268.7403	300	300	260.4044	266.7806527	259.7062335	256.2554544
Pg8 (MW)	295.0226	285.4014	289.0542	299.6063	284.5362	290.8186132	285.8462781	297.0513115
Pg9 (MW)	284.6146	286.4166	288.3886	288.4402	284.6324	284.6025908	284.6018609	299.9953945
Pg10 (MW)	279.6016	205.0934	220.5232	136.1618	204.8627	207.4135385	207.9820774	130
Pg11 (MW)	318.4002	168.8124	243.6735	243.7775	168.3955	243.5827337	243.2637849	169.3090338
Pg12 (MW)	318.4004	168.8851	169.2619	319.3076	243.5983	318.3996454	316.302264	306.094109
Pg13 (MW)	394.2803	394.224	484.0939	304.5266	394.3207	304.5241963	393.3344712	394.5008241
Pg14 (MW)	484.2888	484.035	394.2923	394.2702	484.0415	304.5184491	393.7099759	393.7355999
Pg15 (MW)	484.0382	394.2865	394.2815	394.2756	394.287	394.322214	394.2903111	305.5366609
Pg16 (MW)	304.6382	394.2512	394.4309	394.3378	393.7834	304.521412	394.0107241	394.4500635
Pg17 (MW)	489.6014	489.3601	489.4321	489.547	489.7002	489.2867798	400.1520446	500
Pg18 (MW)	489.2782	489.3589	490.2527	489.3544	399.5418	399.4800955	490.2136591	490.8920464
Pg19 (MW)	511.9256	511.9201	331.7721	421.5186	511.7246	511.432115	511.2793736	514.6259351
Pg20 (MW)	511.3778	511.34	511.3554	511.3658	421.521	511.3041636	511.0039475	525.3542635
Pg21 (MW)	433.5245	525.5076	523.4301	523.3126	525.9069	523.3475504	521.1386228	550
Pg22 (MW)	433.5316	523.5785	433.7107	549.9264	523.3683	523.2824448	523.1449807	548.5299466
Pg23 (MW)	523.2806	523.4343	523.6605	523.4014	523.2229	523.2914355	523.4973647	550
Pg24 (MW)	523.2888	523.7584	523.5275	525.0759	537.5339	523.3169144	532.1422657	521.6137338
Pg25 (MW)	523.2889	523.7573	523.4639	529.0869	523.2575	523.306813	525.425869	522.5635051
Pg26 (MW)	524.059	523.8777	523.6618	524.6181	523.363	523.2792844	524.750045	549.3197361
Pg27 (MW)	10	10.0039	52.0712	10.3208	10.045	10.00833641	14.82149808	14.54018441
Pg28 (MW)	10	10.0903	32.943	11.976	10.0584	10.00401295	17.55317247	10.09827847
Pg29 (MW)	11.2485	10.0012	42.5597	12.0379	10.091	10.02394824	10.15981108	10.90987678
Pg30 (MW)	91.0437	96.9912	96.6457	91.331	95.7828	96.95242919	88.64142595	96.99993948
Pg31 (MW)	189.9732	189.9995	190	190	189.9726	181.241749	167.7277666	180.3914692
Pg32 (MW)	189.9997	189.9932	190	189.994	189.9393	189.9953502	110.3709413	189.8297956
Pg33 (MW)	163.6655	189.9954	190	189.9604	189.9865	159.7499057	189.7311867	181.720502
Pg34 (MW)	165.1037	169.3255	174.713	184.4522	170.7813	199.9449699	154.7321767	199.9999763
Pg35 (MW)	166.7651	199.9967	199.9973	173.6353	199.897	199.6705009	168.5102131	182.9159828
Pg36 (MW)	165.8941	189.6863	167.6098	165.3069	166.564	199.991963	167.5306785	200
Pg37 (MW)	89.7967	110	89.3805	66.2837	90.1237	89.86684403	95.80067815	109.9993619
Pg38 (MW)	109.9979	109.9998	60.2502	109.9931	109.5728	109.9917663	94.59496126	110
Pg39 (MW)	109.9994	109.9919	97.059	109.9853	57.7381	94.16960534	100.4361961	89.83998575
Pg40 (MW)	516.5065	511.4807	421.8636	511.3409	511.31	511.3076161	511.4129671	550
Pg41 (MW)	112.3421	97.1804	157.4488	155.524	146.3775	132.3982552	88.08453564	126.911668
Pg42 (MW)	50.4459	43.397	162.3604	139.4474	112.5172	144.4049507	176.3682171	126.6515375
Pg43 (MW)	131.6591	89.6268	119.564	147.3521	166.6346	88.99398926	133.3407891	115.3838013
Pg44 (MW)	57.3384	45.1847	103.2307	112.9782	101.4222	105.2551322	82.43229679	133.2788296
Pg45 (MW)	10.0991	21.2282	41.2788	65.9401	78.014	93.63589835	84.39909467	42.80196981
Pg46 (MW)	44.2424	48.3113	91.2561	68.5323	102.0881	49.07352085	80.59064342	43.67911921
Pg47 (MW)	103.2198	128.4079	87.1336	40.2656	72.7479	76.78719074	40.12150597	77.28023842
Pg48 (MW)	40.2287	59.2361	56.8732	74.6718	81.453	55.66222673	40.39987198	74.81841571
Pg49 (MW)	127.0797	96.9275	101.7154	161.1207	114.0001	167.415806	128.5747866	99.51927201
Pg50 (MW)	65.5205	56.1951	115.7489	92.7839	115.9933	170.7899652	153.1704573	116.0935991
Pg51 (MW)	20.6157	19.4934	111.1813	131.9444	105.0388	167.4168782	134.9154112	109.3199759
Pg52 (MW)	56.4012	58.3874	146.7759	129.1619	110.138	125.329591	169.0986537	106.0198439
Pg53 (MW)	168.9969	137.1533	54.607	49.6165	58.5187	60.42436073	57.48988444	60.72297981
Pg54 (MW)	40.4449	54.4494	69.7127	46.5981	88.4724	79.5458983	73.5303264	52.58094411
Pg55 (MW)	101.1777	135.4933	73.5156	48.279	90.3362	56.36733616	47.84016687	43.69127173
Pg56 (MW)	55.7835	73.2057	63.6804	68.7759	98.8981	66.27287672	41.59481573	56.18677799
Pg57 (MW)	10.056	22.5826	29.6084	17.0945	11.9271	10.526294	39.568433	12.984927
Pg58 (MW)	64.4182	48.4507	32.8538	20.8543	10.2473	13.966558	30.601921	29.500822
Pg59 (MW)	152.2648	114.4764	24.4815	20.437	10.7945	10.242311	15.455255	10.224582
Pg60 (MW)	56.1164	61.8714	34.4688	23.6739	10.8036	18.416857	28.854667	13.318664

This article has been accepted for publication in a future issue of this journal, but has not been fully edited. Content may change prior to final publication. Citation information: DOI 10.1109/ACCESS.2021.3087449, IEEE Access

TABLE 3. Coninued

Unit	WOA	MPHS	MPOA	IMPOA	MRF	JFSOA	SDO	HBOA
Pg61 (MW)	123.1718	134.5865	87.7235	39.1262	46.0268	46.39822	49.290726	37.731189
Pg62 (MW)	46.9576	58.702	43.6068	52.6339	50.9742	77.241845	74.333519	55.419047
Pg63 (MW)	11.9343	14.2665	71.0358	39.5056	46.4064	53.473728	83.330785	38.524705
Pg64 (MW)	57.1203	45.9687	46.6292	35.7657	81.0028	57.218278	35.547811	58.369607
Hg41 (MWth)	122.389	113.7627	147.6562	146.6201	141.47	133.6418	108.7418	130.36047
Hg42 (MWth)	84.017	77.8321	150.4384	137.5875	122.4835	140.38155	157.70193	130.22022
Hg43 (MWth)	133.2295	109.4936	126.4326	142.0364	152.8414	109.2841	131.03854	123.54322
Hg44 (MWth)	89.9664	79.4565	117.2753	122.7413	116.2061	118.40557	98.006315	134.13526
Hg45 (MWth)	40.0414	44.7352	76.1032	97.3837	107.8045	121.30091	113.23396	77.305255
Hg46 (MWth)	24.2001	26.025	119.2437	99.63	128.5812	82.83207	110.00064	78.021767
Hg47 (MWth)	115.7242	131.1739	115.6884	75.23	103.2457	106.75568	75.067676	107.1827
Hg48 (MWth)	75.1974	91.5396	89.5394	104.929	110.7559	88.52056	75.295738	105.05633
Hg49 (MWth)	130.6574	113.4407	116.4089	149.7545	123.2778	153.28427	125.33879	115.19298
Hg50 (MWth)	97.0303	88.9429	124.3008	111.4069	124.4197	155.14832	145.2591	124.37381
Hg51 (MWth)	44.5495	44.0508	121.7187	133.3892	118.2344	153.29586	135.01731	120.69336
Hg52 (MWth)	29.7277	30.6049	141.5828	131.7908	121.1505	129.39075	154.20294	118.7926
Hg53 (MWth)	154.183	136.0749	87.5945	83.2834	90.9128	92.630772	88.899597	92.889872
Hg54 (MWth)	75.3759	87.4415	100.6428	80.6963	116.7821	109.13766	103.85151	85.79143
Hg55 (MWth)	116.1224	135.2714	103.9151	82.1301	118.4447	89.1249	81.352437	78.186666
Hg56 (MWth)	88.6239	103.6541	95.4345	99.841	125.8343	97.677172	76.35822	88.97404
Hg57 (MWth)	39.7995	45.3681	48.3974	43.0398	40.8103	40.225735	52.660052	41.279683
Hg58 (MWth)	33.3716	25.9449	49.7936	44.6247	40.0514	41.699032	48.821315	48.357485
Hg59 (MWth)	144.7767	123.3418	46.1677	44.4733	40.3305	40.103128	41.545489	40.096243
Hg60 (MWth)	88.9117	93.8406	50.4183	45.8603	40.3306	43.604568	48.016149	41.229832
Hg61 (MWth)	128.4364	134.6699	43.9544	21.857	25.0017	25.175411	26.454331	21.184123
Hg62 (MWth)	81.0055	91.1235	23.9094	27.9878	27.233	39.198929	37.819152	27.168868
Hg63 (MWth)	40.8289	41.6933	36.3734	22.0418	24.4381	28.384611	41.713801	21.602582
Hg64 (MWth)	30.0546	24.7914	21.4939	17.154	40.905	30.097467	13.095769	25.847086
Hg65 (MWth)	383.1144	389.4986	282.7322	327.5015	340.3042	347.86975	334.4616	397.96444
Hg66 (MWth)	59.9997	59.9997	369.2619	390.4617	338.8826	349.52939	394.53059	394.08612
Hg67 (MWth)	60	59.998	386.0055	392.0802	340.7755	349.73186	358.54799	400.20396
Hg68 (MWth)	119.9855	119.9399	367.6143	384.5644	339.2679	344.06369	394.30008	401.44516
Hg69 (MWth)	119.999	119.9995	60	59.9984	59.9823	59.994889	59.69648	60
Hg70 (MWth)	402.653	388.5823	59.9999	59.9836	59.8608	59.977035	59.639208	59.363243
Hg71 (MWth)	59.8978	59.9997	59.9974	60	59.9941	59.992207	59.908384	59.861172
Hg72 (MWth)	59.9998	59.989	59.9976	59.9957	59.9949	59.814627	59.623394	60
Hg73 (MWth)	119.9996	119.8977	59.9994	59.9999	59.9795	59.983075	59.847266	58.883967
Hg74 (MWth)	119.9999	119.9265	60	60	59.9874	59.999159	59.859142	59.541711
Hg75 (MWth)	385.534	385.8941	59.9985	60	59.9795	59.900677	59.848149	59.812732
Hg76 (MWth)	58.9464	59.9999	59.9998	59.9969	59.8799	59.980839	59.705253	60
Hg77 (MWth)	59.9995	59.9967	119.9998	119.9984	119.9313	119.99507	119.87857	120
Hg78 (MWth)	119.7982	119.997	119.9925	120	119.9494	119.99397	119.36566	120
Hg79 (MWth)	119.9988	119.8126	119.9821	119.9984	119.8432	119.99531	114.40442	119.95288
Hg80 (MWth)	381.8642	402.4022	119.9979	119.9414	119.9641	119.93083	119.90201	120
Hg81 (MWth)	59.9999	59.9995	119.9999	120	119.9284	119.95831	119.48437	119.99997
Hg82 (MWth)	59.9991	59.9995	119.9829	120	119.9682	119.99584	119.97149	119.4424
Hg83 (MWth)	119.998	120	119.9556	120	119.998	119.99688	118.70615	119.99989
Hg84 (MWth)	119.9982	119.8582	119.9993	119.9905	119.9835	119.99574	118.82723	111.95649
Sum (Pg)	12700	12700.01	12700	12700	12700	12700	12700	12700
Sum (Hg)	5000.005	5000.064	5000	5000	5000	5000	5000	5000
WFC ($)	290123.97*	288157.43*	294717.7	289903.8	291225.6	290323.82	292788.5	289822.39

This article has been accepted for publication in a future issue of this journal, but has not been fully edited. Content may change prior to final publication. Citation information: DOI 10.1109/ACCESS.2021.3087449, IEEE Access

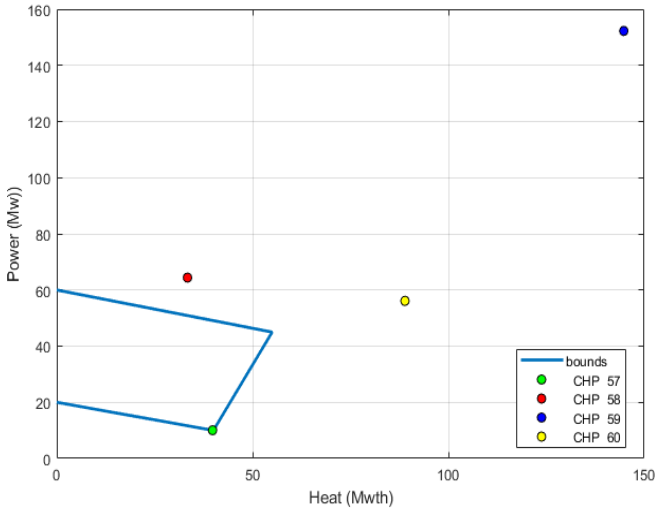

FIGURE 8. Sample of violated operating point of CHP units 57-60 by WOA.

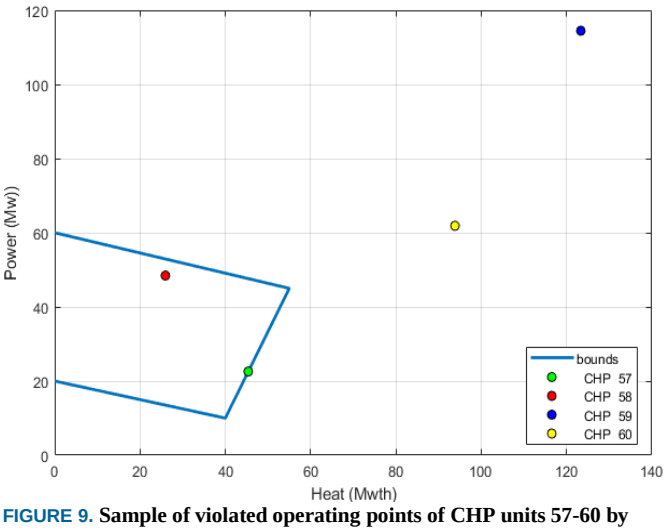

FIGURE 9. Sample of violated operating points of CHP units 57-60 by MPHS.

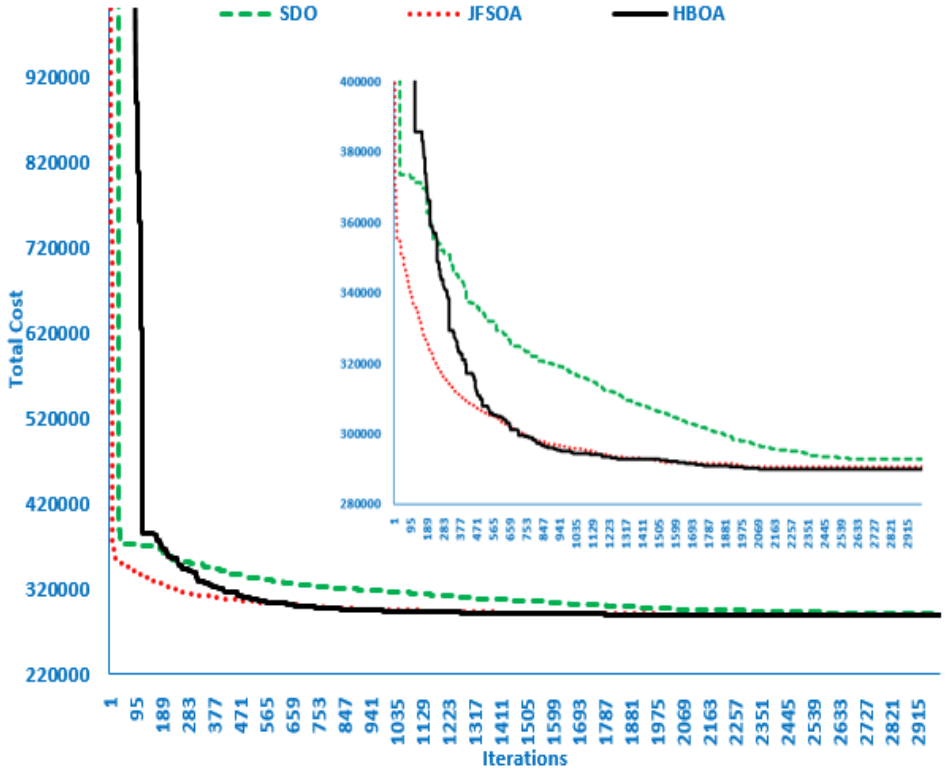

FIGURE 10. Convergence characteristics of HBOA versus other recent optimizaion techniques for the CSED problem of the 84-unit system.

D. SIMULATION RESULTS OF LARGE-SCALE TEST SYSTEM

The 96-unit system represents a large-scale test system, which can be used to assess the scalability, stability and efficiency of the proposed technique. The load and heat demand of this test system are 12700 MW and 5000 MWth, respectively. Additionally, it includes 20 heat units, 52 thermal units, and 24 CHP units as obtained from [7]. Table 4 gives the optimal unit scheduling using the proposed techniques as well as other relevant techniques such as WOA [7], WVO_PSO [12], MRF [40], MPOA, IMPOA, SDO and JFSOA. By simulating the result, it can be observed that the obtained optimal WFC (235102.65 $) achieved by the proposed HBOA is lower than the other reported techniques. The calculated WFC of other techniques WOA, WVO_PSO, MRF, MPOA, IMPOA, SDO and JFSOA are, respectively, 236702.97 $, 235789.2 $, 235541.4 $, 236283.1 $, 235260.3 $, 236185.18 $ and 235277.05 $.

Similar to previous test systems, the operational points for the findings presented in Table 4 by WOA [7] and WVO_PSO [12] are reviewed. This evaluation demonstrates that the operating point supplied by WOA [7] is possible

This article has been accepted for publication in a future issue of this journal, but has not been fully edited. Content may change prior to final publication. Citation information: DOI 10.1109/ACCESS.2021.3087449, IEEE Access

with precise WFC since the difference between its stated and calculated values is negligible. In contrast, however WVO_PSO [12] provides suitable operating point for all units, a significant difference is remarked between the stated WFC value of 235789.2 $ and the computed 238005.79 $.

The convergence characteristics, shown in Fig. 11, ensures that the proposed HBOA is capable to find feasible operating points accurately for all units and to improve the solution quality for such large-scale system.

TABLE 4. Optimal scheduling of the CSED problem for 96-unit system by HBOA and other techniques.

Unit	WOA	WVO_PSO	MRF	MPOA	IMPOA	SDO	JFSOA	HBOA
Pg1 (MW)	361.6989	179.5201	538.5341	628.3176	448.7995	448.7294	628.1374	537.254715
Pg2 (MW)	225.5924	149.7683	224.4012	224.5265	299.2027	224.5646	224.3853	341.5738074
Pg3 (MW)	224.3946	229.3011	299.1921	149.5909	224.4507	149.8704	224.5230	151.1408777
Pg4 (MW)	110.8030	109.8671	109.9002	60.0035	63.4146	109.7272	109.8640	109.0977628
Pg5 (MW)	110.0061	109.8682	109.9178	159.7684	109.7907	160.7416	109.8715	64.10866612
Pg6 (MW)	159.6156	116.8034	109.8556	66.8003	159.8008	159.1329	159.7649	110.0480942
Pg7 (MW)	109.8526	159.7348	109.8524	111.3558	111.3255	114.5665	159.7332	94.33638081
Pg8 (MW)	110.3586	159.7467	109.8904	109.8511	161.0556	109.7220	110.0519	60.00000879
Pg9 (MW)	160.0915	109.8668	159.7286	109.8603	160.0759	109.4680	110.3982	108.2875293
Pg10 (MW)	114.8006	114.8000	77.3946	77.3244	116.7355	87.2949	110.6273	115.4310336
Pg11 (MW)	114.9807	77.4926	77.4030	40.2655	75.2831	79.0857	77.4864	49.01342421
Pg12 (MW)	92.3721	92.4009	55.0881	118.7892	91.1026	92.7083	92.3981	92.02655803
Pg13 (MW)	92.4525	92.4049	92.3770	92.3969	92.4673	92.5555	92.4291	55.18840658
Pg14 (MW)	359.0854	452.2910	449.1396	628.3182	359.0546	359.0618	358.9390	360.9754061
Pg15 (MW)	225.1433	227.3241	224.4004	224.3978	75.3023	220.8337	224.4711	299.3860657
Pg16 (MW)	229.5487	0.0000	149.5993	224.4013	224.4307	299.2436	227.8984	359.9221971
Pg17 (MW)	164.3339	159.7347	109.8854	159.5379	61.8602	109.9312	109.9684	159.7120077
Pg18 (MW)	160.2151	159.7471	109.8918	159.7402	61.3299	159.7770	109.9616	109.3602599
Pg19 (MW)	159.9402	109.8670	109.8124	159.8021	60.5627	109.5956	109.8707	110.4137284
Pg20 (MW)	109.9636	111.7779	109.8538	159.8253	159.7782	159.5821	110.4373	101.8946306
Pg21 (MW)	146.0127	109.8666	155.7131	109.7960	60.0354	159.6577	109.9683	109.8648707
Pg22 (MW)	120.0047	109.8668	109.9640	113.2404	109.9942	162.2520	109.8613	179.4592083
Pg23 (MW)	77.9996	40.1131	77.4163	59.6964	71.2542	78.1863	114.7916	40.13034648
Pg24 (MW)	77.4223	77.4045	77.4663	113.7356	114.7235	80.1193	77.4448	77.22962911
Pg25 (MW)	92.4849	92.4197	92.4246	89.9064	56.5095	89.5740	92.4135	66.61283247
Pg26 (MW)	93.9975	119.9998	55.0084	92.7438	62.1826	92.9623	92.4438	91.02277492
Pg27 (MW)	359.1802	359.0494	359.0726	359.0086	628.3175	359.4461	359.4659	359.4498313
Pg28 (MW)	299.9979	360.0000	299.1270	150.2002	299.3138	150.0325	149.5652	299.4259674
Pg29 (MW)	224.7272	299.2987	224.4124	149.6189	299.2129	299.2876	224.7536	289.8301184
Pg30 (MW)	159.8239	159.7332	159.7033	159.9275	159.9439	109.8718	109.9432	161.92495
Pg31 (MW)	160.1449	109.8760	159.7413	159.6800	165.6381	110.2902	109.7440	107.7669533
Pg32 (MW)	124.3426	113.2579	109.8501	109.9803	159.7031	109.8811	109.8997	159.4640725
Pg33 (MW)	159.7681	159.7332	160.5856	109.9906	149.1821	159.9922	112.3437	162.5783378
Pg34 (MW)	109.9525	60.0000	109.8423	110.0943	159.9684	111.7247	118.7835	159.9001838
Pg35 (MW)	110.0723	109.8666	109.8916	109.4116	109.9135	109.8613	109.9580	60.03756814
Pg36 (MW)	78.0018	77.5396	77.7225	46.7352	40.3663	78.5714	114.8045	113.7051781
Pg37 (MW)	77.4827	77.4056	77.4192	53.6586	44.5586	77.7615	77.4993	114.3819608
Pg38 (MW)	66.6749	92.8907	92.4623	75.0300	55.1223	92.3722	92.6306	94.29271341
Pg39 (MW)	92.4487	92.4059	55.0310	106.6037	57.4248	92.6213	92.3919	92.65458803
Pg40 (MW)	180.3641	359.0391	448.7942	90.1856	538.5549	449.2151	448.8086	448.3942915
Pg41 (MW)	224.5898	299.6630	149.6504	299.1623	224.4471	224.4453	150.3797	297.8196029
Pg42 (MW)	224.4866	227.5653	224.4160	299.2613	312.9394	231.2957	299.2035	146.2329552
Pg43 (MW)	109.6226	110.1121	109.8406	109.8768	60.8300	109.5049	111.2975	110.6346294
Pg44 (MW)	109.8456	109.8666	109.7623	171.5053	72.3844	109.5823	110.3086	161.7767837
Pg45 (MW)	65.8336	159.7363	126.5520	159.7403	109.9107	111.7111	159.5163	61.66518066
Pg46 (MW)	159.6880	109.8794	109.9766	116.2378	60.2285	60.5083	109.8988	108.9737886
Pg47 (MW)	116.6052	159.7332	109.8817	114.3100	113.1684	109.8581	109.9034	110.4947542
Pg48 (MW)	159.2737	159.7339	109.8483	109.8951	159.8220	159.0074	110.2078	109.9050818
Pg49 (MW)	78.0268	76.2477	77.4184	95.4460	111.7253	78.2198	77.3975	42.02833221
Pg50 (MW)	77.5176	77.4035	77.4013	44.6056	45.3943	77.3337	77.3324	72.25178996
Pg51 (MW)	92.8301	92.4021	92.4220	119.9983	92.5237	106.8704	92.7631	93.0608812
Pg52 (MW)	85.2843	92.4705	92.6009	113.3472	63.6064	86.4035	93.1231	92.57317097
Pg53 (MW)	111.0331	82.5222	97.9354	117.3331	104.0096	118.8776	104.9832	104.4403419
Pg54 (MW)	68.5580	68.4792	58.3116	68.6504	67.0915	53.4688	45.1316	47.60359863
Pg55 (MW)	95.6342	119.0174	114.8980	102.2794	83.8374	107.2267	100.2247	88.44497134
Pg56 (MW)	60.8717	88.1603	46.6792	58.7652	50.0228	65.5615	51.7195	50.14389995
Pg57 (MW)	23.7299	10.3817	26.4381	14.1789	24.4103	31.9267	19.0094	12.03402877
Pg58 (MW)	41.3490	45.4655	36.6545	40.9762	36.0253	61.9135	56.3032	45.6270289
Pg59 (MW)	139.9448	118.4227	96.2230	113.1150	115.7964	90.7926	125.4849	91.41295489
Pg60 (MW)	46.8012	71.0473	63.5999	53.7449	64.8510	43.2561	51.9022	51.86266145

This article has been accepted for publication in a future issue of this journal, but has not been fully edited. Content may change prior to final publication. Citation information: DOI 10.1109/ACCESS.2021.3087449, IEEE Access

TABLE 4. Continued

Unit	WOA	WVO_PSO	MRF	MPOA	IMPOA	SDO	JFSOA	HBOA
Pg61 (MWth)	116.4269	101.8515	151.5302	86.5572	117.3994	81.8343	91.1831	110.2162351
Pg62 (MWth)	79.0704	51.5329	77.3787	65.4999	45.0354	59.3903	54.1472	47.62594622
Pg63 (MWth)	33.3173	10.0378	18.0933	24.1485	16.7891	25.694449	34.655934	18.272772
Pg64 (MWth)	59.7067	53.7073	53.0368	43.3566	55.8517	56.936262	75.627888	45.155884
Pg65 (MWth)	100.4416	121.9513	143.9952	112.1218	87.8497	87.130209	148.19343	88.829361
Pg66 (MWth)	74.1967	51.078	42.2496	71.6779	40.3985	42.186016	75.326734	43.74986
Pg67 (MWth)	120.2089	113.1537	109.9469	100.193	116.9941	133.38585	100.58341	95.340679
Pg68 (MWth)	61.1074	62.0878	79.6617	44.4974	56.0185	41.93974	42.252459	67.297804
Pg69 (MWth)	11.0113	11.5777	11.1333	22.2128	24.1531	14.52258	17.202374	11.638244
Pg70 (MWth)	69.0899	60.2592	43.7086	59.5941	38.9905	75.86932	47.915618	35.028678
Pg71 (MWth)	122.8034	175.0835	109.1474	99.2229	99.5488	120.0605	99.938915	87.384128
Pg72 (MWth)	49.235	72.1306	48.6566	41.7852	42.1765	54.261261	67.954604	53.523651
Pg73 (MWth)	115.1764	162.3515	86.7681	119.2587	112.1269	81.155384	88.257959	106.28473
Pg74 (MWth)	43.7841	103.5256	68.0141	81.821	47.7477	72.80805	53.319524	65.916093
Pg75 (MWth)	10.2339	15.3356	11.9507	17.8853	32.1539	37.150914	11.427801	12.449246
Pg76 (MWth)	36.5443	53.933	66.4527	53.6216	35.9992	48.038435	47.191073	35.002312
Hg53 (MWth)	121.6489	105.6543	114.2979	125.1893	117.711	125.89573	118.25717	117.8187
Hg54 (MWth)	99.6187	99.5846	90.7973	99.7322	98.3872	86.623498	79.425882	81.187872
Hg55 (MWth)	112.9517	126.1351	123.8053	116.7319	106.3889	119.40622	115.58344	108.9226
Hg56 (MWth)	92.9964	116.5743	80.764	91.1999	83.6523	97.065314	85.11551	83.024668
Hg57 (MWth)	45.8595	40.1635	47.0447	41.7913	46.1404	49.359884	43.852427	40.490709
Hg58 (MWth)	22.7261	24.7569	20.75	22.7167	20.4638	32.210403	29.679309	24.658925
Hg59 (MWth)	137.7969	125.8014	113.3423	122.8215	124.3203	110.03896	129.76254	109.94761
Hg60 (MWth)	80.8243	101.8014	95.3629	86.8657	96.4468	77.583713	85.274518	83.140535
Hg61 (MWth)	124.6482	116.5017	144.3816	107.9191	125.2277	105.26715	110.51193	120.77066
Hg62 (MWth)	108.7221	84.9557	107.2666	97.0135	79.3429	91.719635	87.148267	81.226938
Hg63 (MWth)	49.9249	40.0162	43.4612	46.0603	42.9032	46.723011	50.561873	39.67663
Hg64 (MWth)	31.1612	28.5033	28.1852	23.7898	29.4584	29.958547	38.46521	23.984424
Hg65 (MWth)	115.7042	127.7816	140.1516	122.2641	108.623	108.20305	142.50587	108.20515
Hg66 (MWth)	104.5144	84.563	76.942	102.3467	75.3435	76.881232	105.49604	77.96514
Hg67 (MWth)	126.7515	122.8444	121.0448	115.5599	124.9926	134.10702	115.78643	112.78318
Hg68 (MWth)	93.2126	94.0672	109.2356	78.881	88.8282	76.66424	76.943631	98.469051
Hg69 (MWth)	40.4142	40.6761	40.4834	45.2319	46.059	41.911104	43.086924	40.664318
Hg70 (MWth)	35.4892	31.4813	23.9564	31.165	21.8116	38.131156	25.870776	18.721909
Hg71 (MWth)	128.2524	157.5991	120.5929	115.0262	115.2096	126.69978	115.42154	106.59216
Hg72 (MWth)	82.9501	102.7366	82.4639	76.5419	76.8665	87.306805	99.131229	86.491633
Hg73 (MWth)	123.9395	150.454	108.0163	126.2709	122.2632	104.24372	108.86068	118.09871
Hg74 (MWth)	78.2418	129.8383	99.1825	111.1027	81.6887	103.31798	86.491059	97.014286
Hg75 (MWth)	39.1403	42.2867	40.3153	43.3791	49.4927	51.36668	40.610943	40.89038
Hg76 (MWth)	20.494	28.6059	34.2964	28.4563	20.4515	25.864199	25.540248	18.353784
Hg77 (MWth)	407.0662	348.9612	391.0097	375.3134	377.6032	403.45436	400.14747	385.57459
Hg78 (MWth)	59.7975	59.995	59.9818	60	59.9931	59.826923	59.999812	59.99772
Hg79 (MWth)	59.9911	60	59.9956	60	59.9998	59.981337	59.922567	60
Hg80 (MWth)	119.2458	120	119.997	120	119.9932	119.96359	119.99872	118.82035
Hg81 (MWth)	119.9549	119.9998	119.9965	119.9983	119.9901	119.43458	119.97171	119.99892
Hg82 (MWth)	390.1828	353.8826	389.1268	396.2707	428.6265	420.97925	402.77116	438.22049
Hg83 (MWth)	59.9729	59.9998	59.9812	60	59.9993	59.990183	59.993989	60
Hg84 (MWth)	59.9805	60	59.9953	59.9995	60	58.276324	59.997954	59.858041
Hg85 (MWth)	119.9912	120	119.9933	120	119.9995	117.79733	119.99343	119.95149
Hg86 (MWth)	119.6621	120	119.6262	120	119.9998	119.9557	119.99908	118.46015
Hg87 (MWth)	368.0236	410.0497	388.0796	400.6778	439.4129	383.92681	399.42417	450.50341
Hg88 (MWth)	59.9905	60	59.9083	59.9985	59.9992	59.689402	59.977283	59.784083
Hg89 (MWth)	59.9849	60	59.992	59.9999	60	59.968445	59.991776	59.830588
Hg90 (MWth)	119.9669	120	119.9921	120	120	119.9354	119.9983	119.99947
Hg91 (MWth)	119.905	119.8377	119.9924	120	119.9998	119.92609	119.99419	118.32769
Hg92 (MWth)	378.9529	323.882	386.2081	409.6858	412.3361	411.99124	398.46975	451.81766
Hg93 (MWth)	59.5063	60	59.9914	60	59.9984	59.908463	59.998636	60
Hg94 (MWth)	59.9907	59.9996	59.9989	59.9996	59.9998	59.996388	59.985181	59.916361
Hg95 (MWth)	119.9904	120	119.998	119.9997	119.9853	118.45831	119.98799	119.99988
Hg96 (MWth)	119.8607	120	119.9958	119.9999	119.991	119.99085	119.99335	119.83914
Sum(Pg)	9400.033	9399.99	9400	9400	9400	9400	9400	9400
Sum(Hg)	5000	4999.99	5000	5000	5000	5000	5000	5000
WFC^R	236,699.15	238005.79 #	235541.4	236283.1	235260.3	236185.18	235277.05	235102.65
WFC^C	236702.97	235789.2	235541.4	236283.1	235260.3	236185.18	235277.05	235102.65

This article has been accepted for publication in a future issue of this journal, but has not been fully edited. Content may change prior to final publication. Citation information: DOI 10.1109/ACCESS.2021.3087449, IEEE Access

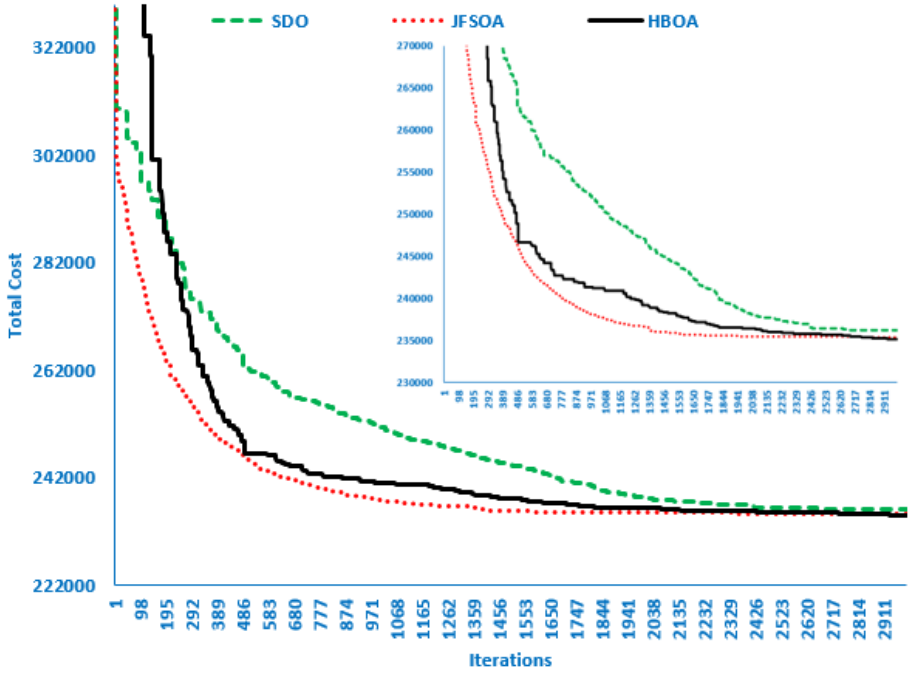

FIGURE 11. Convergence characteristics of HBOA versus other recent optimizaion techniques for the CSED problem of the 96-unit system.

V. CONCLUSION

This paper has been successfully implemented the HBOA for solving the CSED problem. This problem has an economic benefits and reduction of negative environmental effects in case of its optimal solution achievement. HBOA is designed using adaptable penalty formulas to find optimal and feasible operational conditions of heat or power only units and cogeneration combined heat and power units. Based on the infeasible solutions' distance from the next feasible border, it penalizes them with various degrees. Diverse pillars are studied in the CSED issue with inclusion of transmission losses and valve-point effects. HBOA is employed on 4, 24, 84 and 96-unit systems with diverse power and thermal demands. HBOA efficacy for 4-unit and 24-unit test systems is proven. Also, HBOA is applied on the large-scale test systems, 84 and 96-unit test systems, where the results ensure the scalability, efficiency and stability of the proposed techniques as compared with other techniques. In addition, the HBOA success in achieving the optimal solution without any violation of the operating point of any scheduled unit.

ACKNOWLEDGEMENT

This work was supported by Taif University Researchers Supporting Project number (TURSP-2020/86), Taif University, Taif, Saudi Arabia.

References

[1] M. Nazari-Heris, B. Mohammadi-Ivatloo, and G. B. Gharehpetian, "A comprehensive review of heuristic optimization algorithms for optimal combined heat and power dispatch from economic and environmental perspectives," *Renew. Sustain. Energy Rev.*, vol. 81, no. June 2017, pp. 2128–2143, 2018, doi: 10.1016/j.rser.2017.06.024.

[2] M. A. G. Chapa and J. R. V. Galaz, "An economic dispatch algorithm for cogeneration systems," *2004 IEEE Power Eng. Soc. Gen. Meet.*, vol. 1, pp. 989–993, 2004, doi: 10.1109/pes.2004.1372985.

[3] T. G. M. I. Henwood, "An algorithm for combined heat and power economic dispatch," *IEEE Trans. Power Syst.*, vol. 11, no. 4, pp. 1778–1784, 1996, doi: 10.1109/59.544642.

[4] C. Lin, W. Wu, B. Zhang, and Y. Sun, "Decentralized Solution for Combined Heat and Power Dispatch Through Benders Decomposition," *IEEE Trans. Sustain. Energy*, vol. 8, no. 4, pp. 1361–1372, 2017, doi: 10.1109/TSTE.2017.2681108.

[5] A. Sashirekha, J. Pasupuleti, N. H. Moin, and C. S. Tan, "Combined heat and power (CHP) economic dispatch solved using Lagrangian relaxation with surrogate subgradient multiplier updates," *Int. J. Electr. Power Energy Syst.*, vol. 44, no. 1, pp. 421–430, 2013, doi: 10.1016/j.ijepes.2012.07.038.

[6] F. P. Mahdi, P. Vasant, V. Kallimani, J. Watada, P. Y. S. Fai, and M. Abdullah-Al-Wadud, "A holistic review on optimization strategies for combined economic emission dispatch problem," *Renew. Sustain. Energy Rev.*, vol. 81, no. June 2017, pp. 3006–3020, 2018, doi: 10.1016/j.rser.2017.06.111.

[7] M. Nazari-Heris, M. Mehdinejad, B. Mohammadi-Ivatloo, and G. Babamalek-Gharehpetian, "Combined heat and power economic dispatch problem solution by implementation of whale optimization method," *Neural Comput. Appl.*, vol. 31, no. 2, pp. 421–436, 2019, doi: 10.1007/s00521-017-3074-9.

[8] E. Khorram and M. Jaberipour, "Harmony search algorithm for solving combined heat and power economic dispatch problems," *Energy Convers. Manag.*, vol. 52, no. 2, pp. 1550–1554, 2011, doi: 10.1016/j.enconman.2010.10.017.

[9] M. Basu, "Combined heat and power economic dispatch by using differential evolution," *Electr. Power Components Syst.*, vol. 38, no. 8, pp. 996–1004, Jan. 2010, doi: 10.1080/15325000903571574.

[10] B. Deng, Y. Teng, Q. Hui, T. Zhang, and X. Qian, "Real-coded quantum optimization-based Bi-Level dispatching strategy of integrated power and heat systems," *IEEE Access*, vol. 8, pp. 47888–47899, 2020, doi: 10.1109/ACCESS.2020.2978622.

[11] Y. ali Shaabani, A. R. Seifi, and M. J. Kouhanjani, "Stochastic multi-objective optimization of combined heat and power economic/emission dispatch," *Energy*, vol. 141, pp. 1892–1904, 2017, doi: 10.1016/j.energy.2017.11.124.

[12] S. Dolatabadi, R. A. El-Sehiemy, and S. GhassemZadeh, "Scheduling of combined heat and generation outputs in power systems using a new

hybrid multi-objective optimization algorithm," *Neural Comput. Appl.*, vol. 32, no. 14, pp. 10741–10757, 2020, doi: 10.1007/s00521-019-04610-1.

[13] B. Mohammadi-Ivatloo, M. Moradi-Dalvand, and A. Rabiee, "Combined heat and power economic dispatch problem solution using particle swarm optimization with time varying acceleration coefficients," *Electr. Power Syst. Res.*, vol. 95, pp. 9–18, 2013, doi: 10.1016/j.epsr.2012.08.005.

[14] M. Nazari-Heris, B. Mohammadi-Ivatloo, K. Zare, and P. Siano, "Optimal generation scheduling of large-scale multi-zone combined heat and power systems," *Energy*, vol. 210, p. 118497, 2020, doi: 10.1016/j.energy.2020.118497.

[15] M. Liu, S. Wang, and J. Yan, "Operation scheduling of a coal-fired CHP station integrated with power-to-heat devices with detail CHP unit models by particle swarm optimization algorithm," *Energy*, vol. 214, p. 119022, 2021, doi: 10.1016/j.energy.2020.119022.

[16] S. Yadegari, H. Abdi, and S. Nikkhah, "Risk-averse multi-objective optimal combined heat and power planning considering voltage security constraints," *Energy*, vol. 212, p. 118754, 2020, doi: 10.1016/j.energy.2020.118754.

[17] A. Naderipour, Z. Abdul-Malek, S. A. Nowdeh, V. K. Ramachandaramurthy, A. Kalam, and J. M. Guerrero, "Optimal allocation for combined heat and power system with respect to maximum allowable capacity for reduced losses and improved voltage profile and reliability of microgrids considering loading condition," *Energy*, vol. 196, p. 117124, 2020, doi: 10.1016/j.energy.2020.117124.

[18] M. Nazari-Heris, B. Mohammadi-Ivatloo, S. Asadi, and Z. W. Geem, "Large-scale combined heat and power economic dispatch using a novel multi-player harmony search method," *Appl. Therm. Eng.*, vol. 154, no. August 2018, pp. 493–504, 2019, doi: 10.1016/j.applthermaleng.2019.03.095.

[19] P. K. Roy, C. Paul, and S. Sultana, "Oppositional teaching learning based optimization approach for combined heat and power dispatch," *Int. J. Electr. Power Energy Syst.*, vol. 57, pp. 392–403, 2014, doi: 10.1016/j.ijepes.2013.12.006.

[20] B. Shi, L. X. Yan, and W. Wu, "Multi-objective optimization for combined heat and power economic dispatch with power transmission loss and emission reduction," *Energy*, vol. 56, pp. 135–143, 2013, doi: 10.1016/j.energy.2013.04.066.

[21] C. Shang, D. Srinivasan, and T. Reindl, "Generation and storage scheduling of combined heat and power," *Energy*, vol. 124, pp. 693–705, 2017, doi: 10.1016/j.energy.2017.02.038.

[22] M. Basu, "Bee colony optimization for combined heat and power economic dispatch," *Expert Syst. Appl.*, vol. 38, no. 11, pp. 13527–13531, 2011, doi: 10.1016/j.eswa.2011.03.067.

[23] A. M. Shaheen and R. A. El-Sehiemy, "A Multiobjective Salp Optimization Algorithm for Techno-Economic-Based Performance Enhancement of Distribution Networks," *IEEE Syst. J.*, vol. 15, no. 1, pp. 1458–1466, Mar. 2021, doi: 10.1109/JSYST.2020.2964743.

[24] A. M. Shaheen and R. A. El-Sehiemy, "Application of multi-verse optimizer for transmission network expansion planning in power systems," in *Proceedings of 2019 International Conference on Innovative Trends in Computer Engineering, ITCE 2019*, Feb. 2019, pp. 371–376, doi: 10.1109/ITCE.2019.8646329.

[25] A. M. Shaheen, A. M. Elsayed, R. A. El-Sehiemy, and A. Y. Abdelaziz, "Equilibrium optimization algorithm for network reconfiguration and distributed generation allocation in power systems," *Appl. Soft Comput.*, vol. 98, p. 106867, Jan. 2021, doi: 10.1016/j.asoc.2020.106867.

[26] M. I. Alomoush, "Optimal Combined Heat and Power Economic Dispatch Using Stochastic Fractal Search Algorithm," *J. Mod. Power Syst. Clean Energy*, vol. 8, no. 2, pp. 276–286, 2020, doi: 10.35833/MPCE.2018.000753.

[27] M. I. Alomoush, "Application of the stochastic fractal search algorithm and compromise programming to combined heat and power economic–emission dispatch," *Eng. Optim.*, vol. 52, no. 11, pp. 1992–2010, 2020, doi: 10.1080/0305215X.2019.1690650.

[28] T. T. Nguyen, T. T. Nguyen, and D. N. Vo, "An effective cuckoo search algorithm for large-scale combined heat and power economic dispatch problem," *Neural Comput. Appl.*, vol. 30, no. 11, pp. 3545–3564, 2018, doi: 10.1007/s00521-017-2941-8.

[29] D. Zou, S. Li, X. Kong, H. Ouyang, and Z. Li, "Solving the combined heat and power economic dispatch problems by an improved genetic algorithm and a new constraint handling strategy," *Appl. Energy*, vol. 237, no. December 2018, pp. 646–670, 2019, doi: 10.1016/j.apenergy.2019.01.056.

[30] A. Sundaram, "Combined Heat and Power Economic Emission Dispatch Using Hybrid NSGA II-MOPSO Algorithm Incorporating an Effective Constraint Handling Mechanism," *IEEE Access*, vol. 8, pp. 13748–13768, 2020, doi: 10.1109/ACCESS.2020.2963887.

[31] E. E. Elattar, "Environmental economic dispatch with heat optimization in the presence of renewable energy based on modified shuffle frog leaping algorithm," *Energy*, vol. 171, pp. 256–269, 2019, doi: 10.1016/j.energy.2019.01.010.

[32] A. Srivastava and D. K. Das, "A new Kho-Kho optimization Algorithm: An application to solve combined emission economic dispatch and combined heat and power economic dispatch problem," *Eng. Appl. Artif. Intell.*, vol. 94, p. 103763, Sep. 2020, doi: 10.1016/j.engappai.2020.103763.

[33] M. Basu, "Squirrel search algorithm for multi-region combined heat and power economic dispatch incorporating renewable energy sources," *Energy*, vol. 182, pp. 296–305, 2019, doi: 10.1016/j.energy.2019.06.087.

[34] J. S. Chou and D. N. Truong, "A novel metaheuristic optimizer inspired by behavior of jellyfish in ocean," *Appl. Math. Comput.*, vol. 389, 2021, doi: 10.1016/j.amc.2020.125535.

[35] A. Sundaram, "Multiobjective multi-verse optimization algorithm to solve combined economic, heat and power emission dispatch problems," *Appl. Soft Comput. J.*, vol. 91, p. 106195, 2020, doi: 10.1016/j.asoc.2020.106195.

[36] H. R. Abdolmohammadi and A. Kazemi, "A Benders decomposition approach for a combined heat and power economic dispatch," *Energy Convers. Manag.*, vol. 71, pp. 21–31, Jul. 2013, doi: 10.1016/j.enconman.2013.03.013.

[37] A. M. Shaheen, A. R. Ginidi, R. A. El-Sehiemy, and S. S. M. Ghoneim, "Economic Power and Heat Dispatch in Cogeneration Energy Systems Using Manta Ray Foraging Optimizer," *IEEE Access*, vol. 8, pp. 208281–208295, 2020, doi: 10.1109/ACCESS.2020.3038740.

[38] N. Jayakumar, S. Subramanian, S. Ganesan, and E. B. Elanchezhian, "Grey wolf optimization for combined heat and power dispatch with cogeneration systems," *Int. J. Electr. Power Energy Syst.*, vol. 74, pp. 252–264, Aug. 2016, doi: 10.1016/j.ijepes.2015.07.031.

[39] M. T. Hagh, S. Teimourzadeh, M. Alipour, and P. Aliasghary, "Improved group search optimization method for solving CHPED in large scale power systems," *Energy Convers. Manag.*, vol. 80, pp. 446–456, Apr. 2014, doi: 10.1016/j.enconman.2014.01.051.

[40] A. M. Shaheen, A. R. Ginidi, R. A. El-Sehiemy, and E. E. Elattar, "Optimal economic power and heat dispatch in Cogeneration Systems including wind power," *Energy*, vol. 225, 2021, doi: 10.1016/j.energy.2021.120263.